ELSEVIER

Journal of Power Sources 111 (2002) 193–209

JOURNAL OF POWER SOURCES

www.elsevier.com/locate/jpowsour

Review

Role of carbon host lattices in Li-ion intercalation/de-intercalation processes

M. Noel, V. Suryanarayanan*

Central Electrochemical Research Institute, Karaikudi 630006, India

Received 8 March 2002; received in revised form 13 May 2002; accepted 16 May 2002

Abstract

Despite considerable efforts to find other substituents, carbon still remains the only commercially viable negative electrode (anode) material for Li-on batteries. Present work aimed at understanding, characterising and improving the performance of carbon anode materials is reviewed. A brief historical background of developments in carbon host lattices is presented. A wide range of carbon materials from amorphous to highly oriented graphitic materials and the techniques employed in characterisation of the lithium insertion/de-insertion process are outlined. Fundamental investigations of the electrochemical process on natural graphite, as well as highly oriented pyrolitic graphite materials, are then comprehensively reviewed. The problems and prospects of different hard carbon materials which increased battery capacity are then discussed. A variety of new carbon materials and carbon-based composites are also introduced. The critical review ends with an overview of the present status of carbon materials and their role in Li-ion battery systems for different potential applications.
© 2002 Elsevier Science B.V. All rights reserved.

Keywords: Carbon anodes; Lithium intercalation/de-intercalation; Graphite fibres; Mesocarbon microbeads; Hard carbon materials

1. Introduction

Since Sony Corporation introduced lithium-ion batteries to the market in the early 1990s [1], these secondary batteries have seen substantial growth in demand and are the subject of much research and development work for future applications. Quite similar cylindrical and prismatic cells with comparable performance characteristics have been marketed world-wide by several other companies [2–4]. International seminars are bringing together the latest research groups with elaborate progress summaries [5–7]. In the category of cylindrical and prismatic cells used in portable equipment, lithium-ion batteries have already taken over the first position in dollar value terms [2,8,9]. Many research efforts are in progress to develop larger size batteries for space, load levelling and electric vehicle (EV) applications [10–13] and microbatteries for electronic devices [2,14].

In terms of specific capacity, lithium metal should be the best negative electrode (anode) material for any lithium battery. Nevertheless, many safety considerations and dendrite formation which leads short-circuiting limit the use of lithium metal in secondary batteries. A variety of lithium metal composites [15] and novel host lattices such as amorphous tin oxide and TiO_2 [16,17] are being evaluated as anode materials. In terms of practical utility, however, graphite and non-graphite carbon materials are well ahead of all other host materials under consideration. Hence, this review is confined to carbon and related anode materials.

The introduction of carbon as an anode material in lithium-ion secondary batteries has an interesting history (Table 1). Lithium insertion in graphite host lattices from conventional non-aqueous solvents was reported as early as 1976 [18]. Nevertheless, disintegration of the graphite host lattice during intercalation/de-intercalation has remained an unresolved issue. Lithium incorporation by dipping carbon in molten lithium was reported in the early 1980s [19–21]. This anode was coupled to a $NbSe_3$ cathode. Well-characterised LiC_6 was found to function as an anode material in dioxalane solvent. The search for new solvent-supporting electrolyte systems, including polymer electrolytes, would ensure reversible intercalation/de-intercalation which, in turn, would improve the cycle-life of graphite material [22]. Sony Corporation, in a swift move, reported that lithium insertion could also be successfully carried out in disordered-carbon material [23]. This opened up a lot of

* Corresponding author.
E-mail addresses: vidhyasur@yahoo.co.in, sur_2000_99@yahoo.com (V. Suryanarayanan).

0378-7753/02/$ – see front matter © 2002 Elsevier Science B.V. All rights reserved.
PII: S0378-7753(02)00308-7

Table 1
Historical background of different carbon anode materials

Year	Historical background (in bracket, the inventors)	Reference
1976	Electrochemical intercalation of alkali metal cations in organic donor solvents (Besenhard)	[18]
1981	Molten salt battery using LiC_6 as anode and $NbSe_3$ as cathode in dioxalane (Basu)	[19–21]
1983	Polymer electrolyte cells using lithiated graphite as anode in $LiClO_4$/propylene carbonate (PC) (Yazami)	[22]
1985	Introduction of disordered non-graphitized carbon as anode material (Sony Corporation)	[23]
1990	Commercial battery-hard carbon as anode material in Li/MnO_2 couple (Sony Corporation)	[1]
1990	Use of coke as anode material with $LiMnO_2$ as cathode in $LiAsF_6$; ethylene carbonate (EC)/propylene carbonate (PC) (Dahn)	[24]
1993	Introduction of graphitizable mesocarbon microbeads (MCMB) and non-graphitizable vapour grown carbon fibre (VGCF) as anode material (Matsushita Corporation)	[25]

possibilities in terms of carbon material sources and the choice of solvent-supporting electrolyte system. Following a parallel sequence of developments which resulted in the selection of $LiCoO_2$ as the cathode material, Sony Corporation introduced the first, successful, disordered-carbon-based, Li-ion batteries [1]. The search for other hard carbon materials is still continuing [24]. Subsequent work has established, however, that special types of graphite material can also be successfully used as host lattices in practical Li-ion batteries [25].

Extensive literature exists on the chemistry and electrochemistry of carbon materials [26–28]. The general aspects of graphite as a host lattice for cationic and anionic intercalation have also received considerable attention [8,29,30]. In recent times, extensive summaries of research work on Li-ion batteries are becoming available [31–34]. Many experts have reviewed different aspects of carbon materials as host lattices in Li-ion batteries. Aurback and co-workers [31,35,36], e.g. has discussed extensively the decomposition of the solvent-supporting interface on lithium as well as carbon substrates. Yazami [37,38] has also presented an overview of surface transformation during lithium–carbon interactions. Extensive recent research on varieties of hard carbon materials has been evaluated from time to time by Dahn and co-workers [39,40]. Attempts to model the structure of hard carbon materials and their dependence on heat-treatment temperatures (HTTs) are also being made [41]. In a interesting recent review, hard carbon materials prepared from poly(*p*-phenylene) (PPP), B-doped natural graphite material and vapour grown carbon fibre (VGCF) have been compared using experimental studies [42].

In view of the existence of such a vast and continuously growing literature on Li-on batteries in general, and carbon anode materials in particular, it is neither necessary nor possible to provide an extensive and comprehensive survey of the subject. The objective of this present review is to provide a comprehensive and unified outline of the current trends in research that relate to the development of carbon anode materials for Li-ion batteries. An attempt is also made to provide an objective comparison of different types of carbon materials and their strength and weakness in relation to their applicability as practical anode materials. Examination of classical work in this area is included only to the extent that is necessary for providing a broad perspective of the subject. Most references are confined to reports that have appeared in the past 5–6 years. Finally, an attempt is also made to compare different carbon anode materials that have succeeded in reaching different stages of commercial development. The similarity in the overall structural features of these apparently different carbon materials is highlighted.

2. Materials and methods

Li-ion batteries are conventionally called ‘rocking-chair’ batteries because they operate primarily due to the movement of Li^+ ions into and out of host lattices, alternatively, during charge–discharge cycles. As mentioned above, carbon is the anode material and $LiCoO_2$ or related spinal type oxides serves as the cathode material. During the charging process, Li ions move from the cathode material through the electrolyte into the carbon anode material. During discharge, the movement occurs in the reverse direction. A schematic diagram of Li^+ ion movement is shown in Fig. 1(a) [42].

In a practical Li-ion battery, multiple layers of anodic and cathode materials are assembled together with appropriate separators. In typical cylindrical AA cells, the electrodes are bound as a roll with two separators, and the electrolyte fills the gap between the anode and cathode compartments. A schematic diagram of such a cell is presented in Fig. 1(b) [42]. The carbon anode material itself is prepared by dispersing the selected carbon materials along with a binder such as poly(vinylidene fluoride) (PVdF) on a current-collector [42]. The present review concerns the employment and development of such carbon material Li-ion battery systems.

Basically, Li-ion intercalation/de-intercalation is known to occur only in layered structures such as those that exist on natural graphite materials and synthetic graphite materials like highly oriented pyrolytic graphite (HOPG). Because of the limitations observed in the initial stages of development, non-graphitic carbon materials were taken up as alternate host lattices. Typically, a variety of carbon materials with different levels of graphitization can be obtained from any starting material depending essentially on the processing parameters, especially on the HTT.

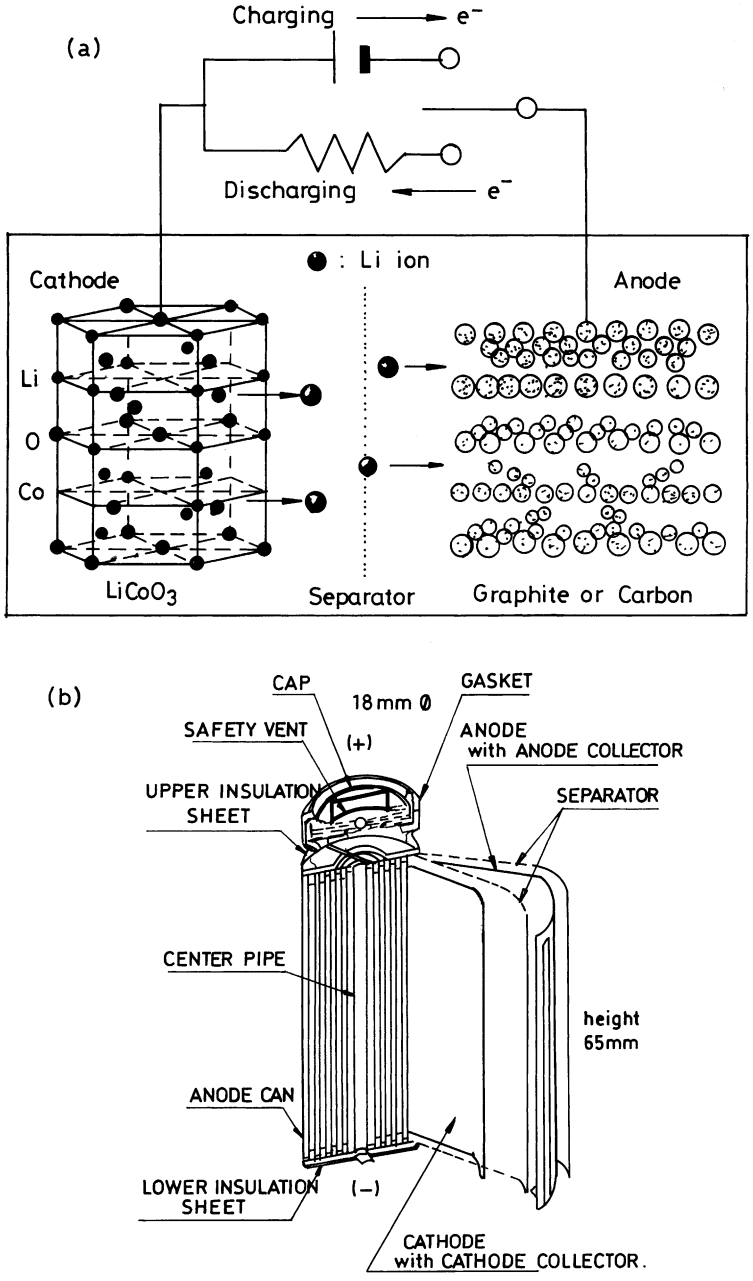

Fig. 1. (a) Charge–discharge mechanism of Li-ion secondary battery and (b) structure of practical cell [42].

Typical reversible capacity values obtained by Dahn et al. [39] from carbon materials heat-treated at different temperatures are shown in Fig. 2(a). Graphite materials obtained with heat-treatment at 200 °C generally have a reversible capacity of 372 mAh g^{-1} (LiC_6 composition). The charge–discharge process does not exhibit significant hysterisis as shown by plot A in Fig. 2(b) [39].

Soft carbon materials are generally heat-treated beyond 700 °C. These carbonaceous materials contain considerable hydrogen as C–H bonding and can take large quantities of Li ions and, hence, possess very high capacity (plot B, Fig. 2(b)). During discharge, however, the materials exhibit considerable overvoltage or voltage loss and, hence, are not suitable for battery applications.

Hard carbon materials obtained in the HTT range 800–1200 °C generally contain much less hydrogen. They essentially consist of non-graphitized carbon platelets. These materials generally possess high irreversible capacity during the first cycle and also higher reversible capacity in subsequent cycles (plot C, Fig. 2(b)).

The extensive research reported in the literature on carbon materials may be classified into three groups. Basic studies are mainly carried out using HOPG or natural graphite material. These studies throw light on many fundamental

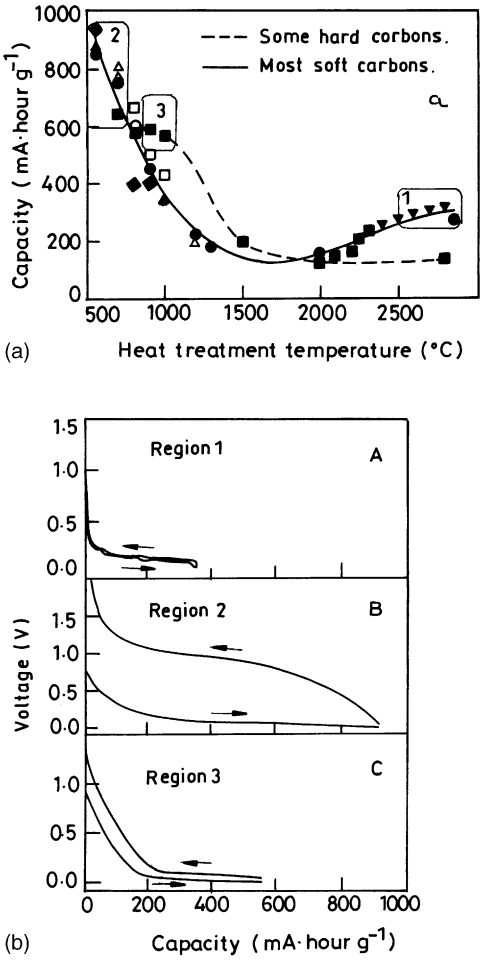

Fig. 2. (a) Plot of reversible capacity for lithium vs. heat-treatment temperature (HTT) for a variety of carbon samples (open symbols, hard carbons; solid symbols, soft carbons). (b) Voltage vs. capacity for (region A) synthetic carbon (region B) petroleum pitch heat-treated at 500 °C (region C) resole resin heat-treated at 1000 °C. These data are for second cycle of Li-carbon test cell [39].

questions relating to graphite intercalation chemistry (Section 3). For practical applications, a number of modified graphite materials are now employed. The modifications of natural graphite or synthesis of new graphite materials or composite materials and their characterisation for battery applications constitute the second major area of research activities (Section 4). There is still considerable interest in improving the hard carbon materials for battery applications. This field indeed throws up new questions and challenges in understanding the nature of intercalation/de-intercalation processes on such materials (Section 5).

Ultimately, the utility of selected carbon materials is determined by their stability, charge–discharge cycling efficiency and reversible charge capacity. This is essentially measured by cycle experiments. Typical charge–discharge curves are shown by plots A–C in Fig. 2(b) [39]. In these studies, lithium metal itself is used as the counter electrode as well as the reference electrode. Hence, the potential is reported with respect to a Li/Li$^+$ reference system. For a practical battery assembly, the Li/Li$^+$ electrode is replaced by the actual cathode material. Such batteries and their characteristics are discussed in the final section of this review (Section 6).

Apart from charge–discharge curves, a wide variety of electroanalytical techniques are commonly employed to characterise the electrochemical processes which occur at the carbon electrode|electrolyte interface (Table 2). Slow-scan cyclic voltammetry (SSCV) is used to determine different stages of the intercalation of lithium ions in graphite and the total charge involved in each stage and the potential of charge–discharge [35]. The information obtained from SSCV on stage phenomena is much more detailed than that obtained from galvanostatic charge–discharge curves. The increase or decrease in the mass during intercalation/de-intercalation is accurately determined by means of an electrochemical quartz crystal microbalance (EQCM) [43]. The interfacial properties of the solid–electrolyte interface (SEI), such as its conductivity and the diffusion rate of ionic species through the interface, are usually determined by employing electrochemical impedance spectroscopy (EIS) [44].

XRD measurements are essentially employed to ascertain the level of intercalation and exfoliation of the graphite lattices on co-intercalation of solvents. Advanced techniques are now available that can determine the spatial distribution of ionic species [35,45–47]. The thermal stability of the intercalated carbon material and the decomposition temperatures for processes such as solvent evaporation and lattice transition can be evaluated using thermo-gravimetry (TG). Differential thermal analysis (DTA) provides further information on the exothermicity and endothermicity of the processes involved [48,49] (Table 2).

Scanning electron microscopy (SEM) is extensively used to evaluate the structure of the carbonised material before and after the intercalation processes [50,51]. The spatial distribution, such as the surface thickness of different elements, may be evaluated by means of transmission electron microscopy (TEM) [52,53]. Scanning tunnelling microscopy (STM) has been employed to assess the level of exfoliation caused by different solvents [54,55]. Atomic force microscopy (AFM) has proved useful in studying the surface transformation as well as the SEI [37,56]. The structure and composition of the SEI formed on carbon anodes is an important aspect. Aurback and co-workers [35,36] have extensively used Fourier transform infrared spectroscopy (FT-IR) to determine the decomposition of the products obtained in different solvents and supporting electrolytes under the operating conditions of Li-ion batteries. There is a vast amount of literature on this subject [31]. The SEI can also be investigated by temperature-controlled gas chromatography (GC) followed by mass spectrum (MS) studies [57,58]. Both intercalation and de-intercalation processes and formation of a fairly thick SEI involve roughening of electrode surface. Such rough electrodes are

Table 2
Different instrumentation techniques employed for characterisation of Li-ion batteries

Analysis	Technique	Reference
(I) Electrochemical		
Charge–discharge and cycling efflciency	Charge–discharge curves	–
Stages of intercalation/reversibility/charge	SSCV	[35]
Mass changes during polarisation	EQCM	[43]
Kinectics of intercalated/de-intercalated process	EIS	[35,44]
(II) Diffraction		
Crystallinity of different stages during intercalation	XRD	[35,45–47]
(III) Thermal studies		
Thermal stability and thermodynamics of intercalated material	TG and DTA	[48,49]
(IV) Microscopic		
Structural changes in electrode material before and after intercalation	SEM and TEM	[50–53]
Morphological changes at sub-micron level	STM and AFM	[37,54–56]
(V) Spectroscopy		
Composition of SEI film	FT-IR and GC–MS	[35,57,58]
Structural disorder of electrode materials	Raman	[59]
Chemical states of intercalants	XPS	[60,61]
Li-ion binding in carbon lattices	^{7}Li NMR	[62,63]

amenable to study Raman spectroscopy. A comprehensive review on this subject is also available [59].

X-ray photoelectron spectroscopy (XPS) is used to evaluate different atomic level bonding interactions during the intercalation process [60,61]. The interactions between Li ions and host lattices under different experimental conditions are now being evaluated using ^{7}Li NMR spectroscopy [62,63]. In what follows, the present level of understanding on the intercalation/de-intercalation behaviour of different types of carbon materials is summarised.

3. Graphite materials

3.1. Natural graphite

As mentioned earlier, intercalation/de-intercalation studies have been mainly carried out on natural graphite material and these studies are still in progress. Comprehensive reviews on many of these aspects are available [35,36,38]. Here, only a brief introductory overview and discussion of some of the latest developments in the field are presented.

Typical slow-scan cyclic voltammograms obtained on natural graphite electrode material are presented in Fig. 3 [35]. The voltammograms clearly indicate the different potential regions which correspond to stage transitions on graphite electrodes. It is noted from these data that in such graphite material, all the intercalation/de-intercalation processes proceed within a potential range of 300 mV versus Li/Li^{+}. This explains the excellent discharge potential values available from graphite-based Li-on batteries.

The allotropic modifications of graphite material also appear to play an important role in intercalation/de-intercalation efficiency (IDE) and cycle efficiency. The rhombohedral form is stable at lower temperatures, and therefore, exhibits better structural stability and cycle-life [64].

Despite extensive basic studies, natural graphite flakes have not been employed in commercial carbon anodes. Many factors contribute to the limitations. Only the edge plane fraction of the natural graphite flakes contribute to the intercalation/de-intercalation process. A direct correlation is found between the basal plane fraction and irreversible

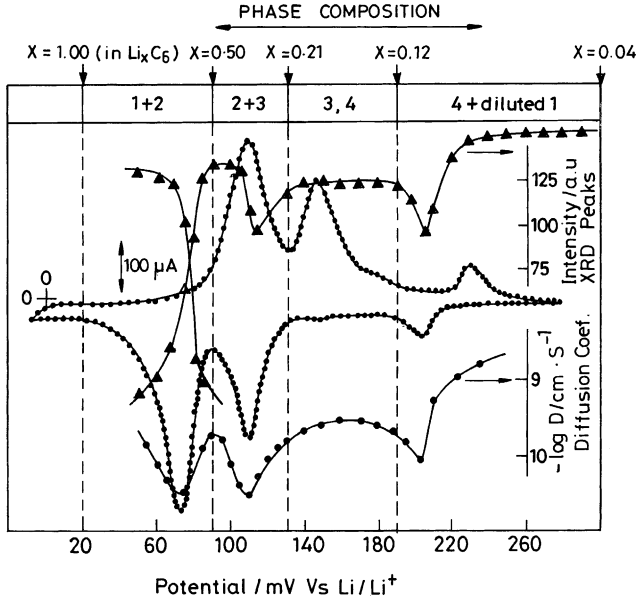

Fig. 3. Potential dependence of chemical diffusion coefficient of lithium into graphite calculated from intensity of major XRD peaks (e.g. 0 0 2 and 0 0 4) during intercalation, and a complete slow-scan rate cyclic voltammogram of a thin (10 μm) composite graphite electrode (KS-6 from Lonza) in EC–DMC/LiAsF$_6$ [31].

capacity [65]. Methods for determining the effect of the basal plane fraction on natural graphite flakes have also been described in the recent literature [66]. Higher porosity also leads to higher irreversible capacity. Pore diameter sizes of 2–50 nm are found to cause capacity loss [67].

It is now well known that decomposition of propylene carbonate (PC) is quite severe on graphite material during the charging process. Intercalation of solvated Li^+ species leads to severe exfoliation and lattice damage. Ethylene carbonate (EC) seems to inhibit co-intercalation of solvent to a significant extent. To overcome other limitations, solvent mixtures containing EC-based electrolyte is now recommended for Li-ion batteries. Although solvent mixtures containing two solvents are usually employed, some studies even recommend four solvent mixtures for higher efficiency [68]. Fluoro ethylene carbonate (FEC) [69] and ethylene sulphite (ES) [70], for which structural similarity with EC is apparent, are also found to be efficient solvents. ES also provides good oxidative stability to the intercalated system [70].

The replacement of toxic $LiAsF_6$ by $LiPF_6$ was a major step towards the commercialisation of Li-on batteries. Further efforts towards finding better lithium salts for Li-ion batteries are also reported from time to time. In EC + PC mixtures, e.g. $LiClO_4$ is found to be effective [71]. In EC solvents containing dimethyl carbonate (DMC) medium, the relative efficiencies of lithium triflate (LiTF) and lithium ammonium triflate (LiTFSI) have been compared. Both these salts are found to exhibit better stability than $LiPF_6$ [72]. A variety of gel or polymer electrolytes are also being investigated for Li-ion batteries. Poly(acrylonitrile) (PAN)-based polymer electrolytes now appear to have an edge over other systems [73].

During the charging process, the electrode potential reaches highly negative values that are quite close to the equilibrium potential of Li/Li^+ itself. The Li^+ ions can be reduced to lithium metal at these potentials. The lithium metal would naturally interact with the solvents, trace levels of water, dissolved CO_2, and any other impurities. In addition to those intercalating through the graphite lattice, the process other than intercalation naturally leads to the formation of a solid film, the SEI, which contains inorganic salts such as LiO and Li_2CO_3 as well as organic salts which involve the decomposition of organic solvents and even polymeric materials.

Aurback et al. [74] have carried out extensive studies of the influence of different operating parameters on the formation of the SEI. Three types of SEI have been identified, as shown in Fig. 4 [74]. In PC, a highly porous and thick SEI is formed. This results in a very high value of irreversible capacity (Fig. 4(a)). The useful reversible capacity in this case is extremely low. In methyl formate (MF), the film porosity and thickness is slightly lower and, hence, a reasonable capacity is observed (Fig. 4(b)). In a EC/DEC mixture, a very thin and compact SEI is formed with fairly low irreversible capacity (Fig. 4(c)).

Considerable attempts have been made to characterise the SEI under widely different experimental conditions [31,57,58]. A wide variety of surface analytical tools are currently employed to obtain further insight into this phenomenon. For example, TEM has been employed to examine the effect of supporting electrolytes [75] and other dissolved impurities [76]. A combination of techniques, including AFM, SEM, DSC [77] and Raman spectroscopy have been employed to study the surface roughness and molecular species found at different stages of electrode polarisation. Recently, thermally programmed GC–MS has been used to determine the decomposition of products and their decomposition temperatures [57,58]. These studies indicate the formation of a predominantly organic film at low current density and a composite inorganic/organic film at higher current density.

A comprehensive understanding of the overall intercalation/de-intercalation process, Li-ion migration in the film, electron transfer kinetics and diffusion of Li^+ species into the lattice may be achieved by means of EIS [78–80]. This technique has also been used to study the effect of charge/discharge cycling on the overall performance [35]. Recently, an investigation has been conducted on the influence of the level of Li^+ species in the host lattice (x in Li_xC_6) on the overall intercalation processes, particularly for improving the diffusion coefficient [44]. A three-electrode assembly is recommended to eliminate the film effects of the Li counter electrode conventionally used in impedance studies. EIS may also be employed to obtain information of practical interest using conventional equilibrium circuit models. Formation of the SEI at room temperature by initial charge–discharge cycling is recommended for subsequent high-temperature operations based on EIS studies.

3.2. Highly oriented pyrolytic graphite (HOPG)

HOPG electrodes may indeed be considered as a better model of graphite material since the electrochemical process can be studied systematically on the basal plane or on the edge oriented plane by proper alignment of the working electrode. It is interesting to note that Basu [21] has employed HOPG as an anode material in one of the initial battery systems developed with LiC_6 [21]. By pyrolysed dipping of HOPG in molten lithium, a very high level of lithium insertion, up to LiC_2 can be achieved. The bonding, reactivity and applicability of such materials, however, are totally different.

It is well known that fluoride intercalation in HOPG only proceeds through the edge plane. The influence of solvent-supporting electrolytes on HOPG is quite similar to that on natural graphite material. The use of PC leads to thicker film formation and surface damage. Even trifluoro propylene carbonate (TFPC) causes significant porous film formation [55]. STM studies in EC/PC mixture have been employed to estimate the level of exfoliation during Li-ion intercalation [54]. Comprehensive studies have been made on the influence of different operating parameters of the SEI formed on the basal and edge planes. The SEI on the basal plane is normally

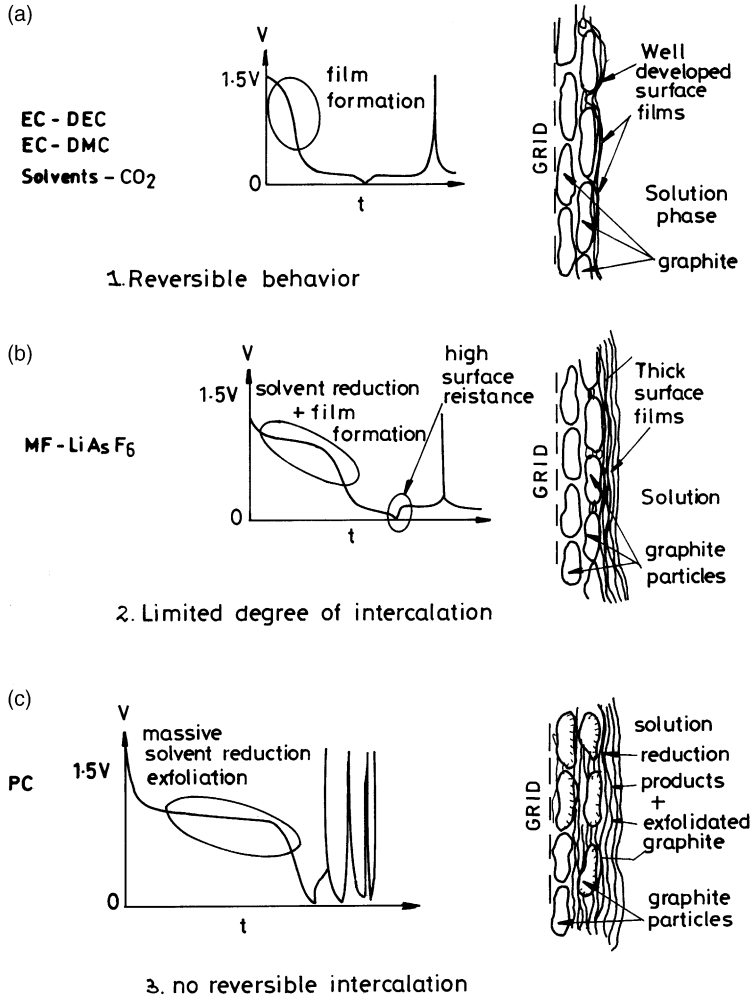

Fig. 4. Typical chrono-amperograms and schematic view of structure of lithiated graphite electrodes in three classes of electrolyte: (a) reversible; (b) partially reversible (low capacity $x < 1$); (c) irreversible behaviour [31].

thinner and is caused predominantly by the decomposition of solvents. By contrast, the SEI on the edge plane is thicker and more porous, is caused mainly by the decomposition of supporting electrolytes, and also contains mostly inorganic salts [60]. More detailed evaluation of the SEI formed on the edge plane has been reported recently [81]. It is interesting to note that use of $LiAsF_6$ [60] and $LiPF_6$ under otherwise identical experimental conditions leads to similar results. The kinetics of electron transfer and diffusion of Li^+ into the HOPG matrix has been investigated using EIS. The impedance tends to increase with increasing intercalation potential [82]. More detailed kinetic studies involving individual stage transitions suggest that during some of the transitions, nucleation of the denser phase is the rate-determining step [83,84].

4. Modified graphite materials

The main cause for the limited success of natural graphite material appears to be the large crystal size with substantially higher L_c as well L_a values. The intercalation/de-intercalation requires movement of Li ions in a number of spatially packed graphene layers, travelling over longer distances. Obviously, the probability of irreversible surface damage becomes higher. A variety of strategies have been adopted to modify graphite materials in order to overcome this difficulty. The most successful of these attempts appear to be the use of mesocarbon microbeads (MCMB) (Section 4.1) and graphite fibres (Section 4.2). Simple reduction of particle-size by ball milling has also been attempted. A few other attempts at surface modification have been reported from time to time (Section 4.3). Recently, there has been tremendous interest in developing new graphite composites for potential application as anode materials in Li-on batteries (Section 4.4).

An interesting recent study reports commonly used graphite particles in Li-ion batteries prepared from coal-tar pitch according the procedure described in a patent [85]. Four common forms of carbon particles namely MCMB, fibres, fakes and potatoes. It should be noted that the common L_c and L_a values range around 20 and 50 nm, respectively. The average particle-size of these materials is in the 2 μm range.

MCMB and fibres are the two most successful systems, and have thus, received considerable attention in the literature. These materials have also been characterised over a wide rage of HTT covering soft carbon to graphite regions. In this section, the entire HTT range is covered.

4.1. Mesocarbon microbeads (MCMB)

Detailed procedures for the preparation of MCMB and their characterisation are well documented in the literature [86,87]. MCMB heat-treated at 70 °C exhibits fairly high capacities of up to 700 mAh g^{-1}. In this soft carbon material, however, the potential of charge varies widely up to 1.2 V. Though the presence of cavities in these materials at low temperatures are suggested as the cause for much higher capacity [88,89], it is not possible to rule out the involvement of different types of bonding. ^{7}Li NMR data obtained on MCMB materials indeed confirm the presence of ionic bonding in these soft carbon materials [62].

For use in a high-voltage battery, the discharge potential of an ideal carbon anode should fall in the range 0–250 mV versus Li/Li^{+}. This is indeed observed for graphitized MCMB [62,88,89]. The discharge mechanisms and the nature of the Li^{+} lattice bonding are quite different in this potential range and beyond [90]. The turbostratic disorder within the microbead is an important factor that contributes to more efficient charge–discharge cycles [90]. As in the case of natural graphite, solvent mixtures containing EC are best suited for battery applications [90,91]. Cyclic voltammetry has also been used effectively to study the stages of Li insertion as well as the intercalation kinetics [91].

Modification of graphitized microbeads in oxygen atmosphere and subsequent annealing in argon was found to increase the irreversible capacity [92]. Compared with sugar-based, hard carbon materials, MCMB shows less irreversible capacity [93]. A similar comparison of irreversible capacities of MCMB, natural graphite, petroleum coke and pitch coke materials, again indicated the very low level of irreversible capacity for MCMB [94]. Among graphitic materials, low crystallinity and minimum surface-area due to the spherical nature of the particles appear to be the advantageous features of MCMB [94].

The structure and composition of the SEI has also received some attention [95]. The low surface-area of MCMB naturally leads to minimum irreversible capacity due to the SEI [95]. The structure and composition of the SEI have been studied by MS [96]. The kinetics of charge-transfer measured by EIS are quite similar to those observed for natural graphite [97]. Though different binders do not influence the performance of MCMB-based carbon anodes, PVdF generally appears to be the binder material of choice [98].

4.2. Graphite fibres

Fibres are the second type of materials that have proved to be successful negative electrodes in Li-on batteries. They are either prepared from pitch-based slurries or vapour grown as carbon fibres. Experimental parameters such as the viscosity of spinning fluid have been optimised to achieve maximum efficiency [51]. Similar optimisation studies have also been reported for vapour grown carbon fibre (VGCF) [99,100]. The fibre size and the method of preparation are found to influence the efficiency of the electrodes substantially. Natural graphite as a minor additive improves the conductivity of graphite fibres and, hence, their efficiency [101]. The graphite material can take different morphological structures depending on the preparative conditions. Radial texture with a zigzag graphite-layer has been found to show minimum exfoliation and high charge–discharge efficiency [102].

Sophisticated instrumental techniques have also been used to examine the intercalation/de-intercalation behaviour of graphite fibres. EIS studies have explained the variation of diffusion coefficient with increasing level of lithium-ion intercalation [103]. A detailed ^{7}Li NMR study on VGCF shows different types of Li–graphite interaction. From the pure ionic lithium stage (0 ppm) to the Li–Li metallic bond stage (262 ppm) (Fig. 5) there is a shift in ^{7}Li NMR peaks for different stages of Li–graphite intercalation [63]. Both MCMB and graphite fibres have been employed in commercial Li-ion batteries. These aspects are discussed in Section 6.

4.3. Graphite powders and surface treatment

Apart from the two types of graphite materials mentioned above, different graphite-powders obtained from different

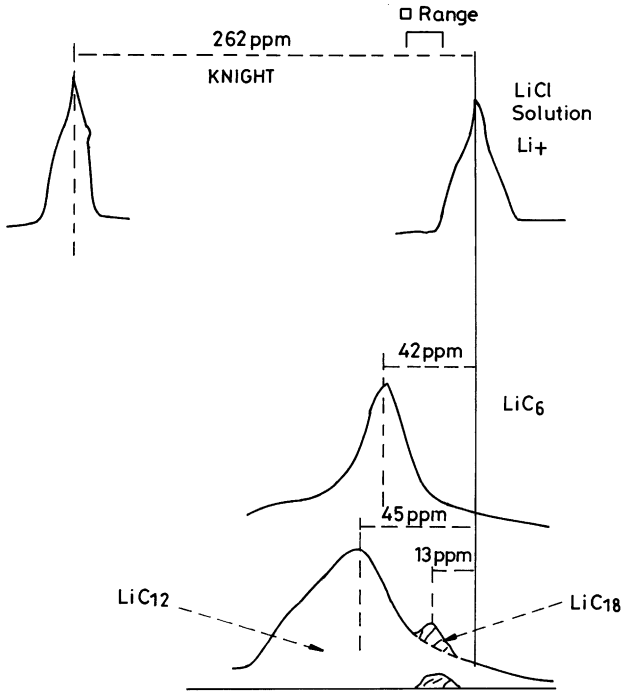

Fig. 5. Position of central peaks of ^{7}Li NMR of LiC_6, LiC_{12} and LiC_{18} as well as metallic lithium [63].

sources, modified by different techniques have been evaluated for potential application as host lattices for intercalation of lithium ions. Powdered coke, graphitized at different HTT, has been evaluated. Both the particle-size [104] and HTT [105] show considerable influence on intercalation/de-intercalation efficiency. The porosity and packing density of graphite particles are also important [104]. Graphite particles obtained from heat-treated gas cokes show lithium-ion interactions which depend on grain size and over all BET surface-area [106].

Mechanical grinding of graphite particles leads to significant changes in their intercalation/de-intercalation behaviour. Different types of milling operations such as jet milling and turbo milling appears to influence the electrode performance differently [107]. In general, milling can lead to the following modifications:

(i) bond-breaking of graphene layers which leads to smaller particles with larger BET surface-area [108];
(ii) expansion of graphite-layer interspacing which results in thinner graphite lattices [108].

These two effects are schematically represented in Fig. 6. The particle-size should be in the optimum range so that irreversible capacity is minimum and both the reversible capacity and the discharge efficiency are maximum [108,109]. More detailed characterisation of ball-milled graphite and size effects are also available [110]. For better performance, ball milling is recommended after HTT and graphitization of coke [111]. For the more active rhombohedral content of graphite materials, further HTT decreases the intercalation efficiency while ball milling improves it [112].

Impure natural graphite particles can be activated by acid treatment [113]. In addition to removing the ash content, slight expansion of graphite inter layer spacing is also achieved with this treatment [113]. Graphite particles can also be cleaned at high-temperature in presence of argon, followed by burning [114].

Slightly expanded graphite lattices allow efficient intercalation/de-intercalation of lithium ions. This may also be achieved by potassium de-intercalation/intercalation in the first cycle [115]. Formation of graphite oxides followed by pyrolytic decomposition in hydrogen atmosphere leads to an exfoliated graphite lattice. With this process, however, irreversible capacity also increases substantially [116].

4.4. Graphite composites and other materials

A wide variety of additives, which range from non-graphitic carbon materials to polymers, gels, host materials and metals, have been added to natural as well as synthetic graphite to improve electrode performance. Forming a thin layer of acetylene black and natural graphite on graphite fibres blocks the active centre, and thus, reduces the irreversible capacity and increase the cycle efficiency [117]. A similar improvement was also observed when synthetic graphite was coated with coke through a slurry process [118].

Another interesting way of controlling active surface sites and improving the intercalation/de-intercalation process is

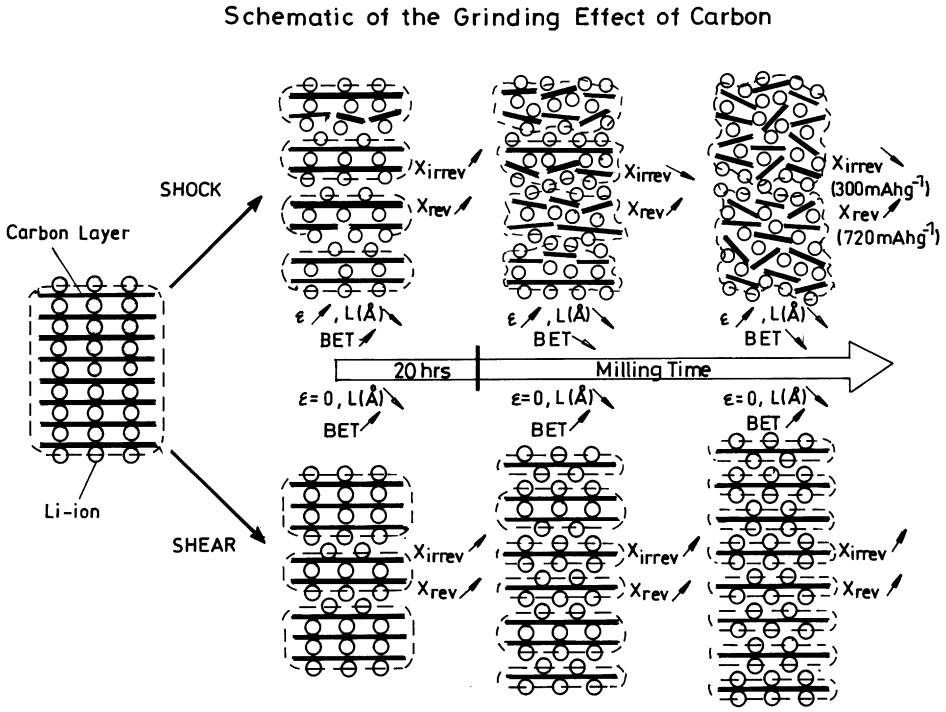

Fig. 6. Proposed scheme describing the effect of the nature of mechanical grinding on carbon powders [108].

coating the graphite particles with polymeric materials [106]. A thin gelating layer, e.g. substantially reduces the thickness of the SEI and, hence, improves the efficiency of graphite anode [119]. Other poly electrolytes including poly(aniline) also exhibit a similar positive influence [120]. Siloxanes can be chemically bonded on the graphite surface to achieve lower irreversible capacity and higher efficiency. This procedure has been reported recently [121,122]. In general, the total weight of the polymeric film should be around 2% of the total weight to ensure higher capacity.

Boron-doped graphite materials have received considerable attention because this process improves the crystallinity of graphite considerably [123]. The doping process itself, however, requires considerable control since formation of lattices with BC or BN structures show wider discharge potentials and hysterisis [124]. Such compounds were specifically synthesised and characterised by earlier workers [125,126] who also confirmed the lower efficiencies of these materials. Further studies of such composite materials demonstrated a lower capacity of 150 mA g^{-1} [127]. The effect of boron doping on MCMB has also been reported [128].

The incorporation of silicon up to 11 wt.% was found to give higher capacity within a wider potential range of 0.1–0.6 V versus Li [129]. A similar improvement was also observed when incorporating V_2O_5, another known host lattice for lithium insertion [130]. Inclusion of tin and SnO increased both the reversible and the irreversible capacities [131]. Dispersion of 13.6 wt.% SnO, e.g. gave an initial irreversible capacity of 450 mAh g^{-1} with a loss of 12% after 30 cycles [132]. Despite the large volume of work on such doped composite materials, their utility as an improved anode material has yet to be established.

Doping graphite with metals such bismuth, gold, palladium and tin was also found to improve the charge–discharge capacity of graphite materials [133]. Among the metal studied, silver, tin and zinc were found to be the most efficient [134]. The improved efficiency was attributed to modification of the SEI found on the surface of the respective metals.

Incorporation of copper and nickel was found to be effective in improving the cycle-life of graphite materials. This is attributed to the suppression of the influence of trace levels of water and oxygen impurities [135]. Copper can also be deposited on to graphite materials by electroplating [136]. Even deposition of CuO or NiO appears to impart beneficial effects [137].

5. Non-graphitic carbons

Graphitization of carbon requires prolonged HTT around 2800 °C which consumes a considerable amount of energy. Non-graphitic carbon materials require much lower HTT and, hence, much less energy consumption. This, coupled with the general trend of higher charge–discharge capacity of hard carbon materials at least during the first few cycles has made hard carbon an attractive anode material for Li-ion batteries. The first successful commercialisation of hard carbon by Sony Corporation [1] has, thus, resulted in extensive research in different laboratories that is aimed at new and improved hard carbon materials. A variety of mineral, agricultural and polymeric sources were employed for preparing these new materials [31,39].

5.1. Carbon materials from petrochemical sources

Petroleum coke was one of the non-graphitic materials which received considerable attention in the early 1990s [24]. The performance of petroleum coke was found to be quite comparable with natural graphite. Apart from the SEI, irreversible interaction of lithium ions with the host lattice was also found to contribute to the irreversible capacity [24]. The diffusion of Li ions into microcavities and the graphene inter-layer spacing has been examined by means of studies [138]. The SEI structure and composition has been determined, in organic carbonate solution over different potential regions using a variety of techniques [139,140].

Petroleum coke modified by meso-phase carbon (MPC) coating gave an increase in the reversible capacity from 170 to almost 300 mAh g^{-1} [141]. Detailed investigations of the intercalation of lithium ions this coated material have also been reported [142].

The next classification is meso-phase, pitch-based carbon fibres. These materials show good reversibility [143] and substantial excess lithium up to a ratio of Li_6C_6 can be loaded [144]. A multi-layered lithium phase incorporated into the carbon fibre has been proposed as the structure of these highly lithiated materials [144]. HTT plays an important role in the charge–discharge characteristics of carbon fibres [145,146]. In general, Q_{irr} capacity decreases up to 1200 °C along with a decrease in H:C atomic ratio. There is a corresponding increase in reversible capacity [145,146]. Anistropic carbon materials are also found to exhibit better reversible capacity.

In contrast to graphitic material, the mechanism of lithium insertion into carbon materials remains an open question. At least, three types of interaction between lithium and the host lattice have been suggested, namely, interaction with graphene layers, surfaces of the poly-nuclear aromatic planes, and lithium insertion in the microscopic spaces at the edges of carbon materials [147]. ^{7}Li NMR has once again been used to distinguish different types of bond between lithium and the host lattice [148]. Such material should indeed be considered as a hybrid of non-graphitic and graphitic regions. ^{13}C NMR has been used to study the crystalline regions of such carbon materials [149].

Oxygen and sulphur impurities present in the carbon fibres have been found to have negative effects on the charge–dischare characteristics [150]. Carbon fibres coated with epoxy resins [151] or quinoline [152] have been found

to show considerably low irreversible capacity. Attempts have also been made to evaluate the performance of boron-doped carbon fibres [153].

5.2. Carbonaceous material from resin and polymers

Dahn and co-workers [154,155] have studied the properties of carbonaceous materials prepared from resins. An increase in reversible lithium insertion with HTT was attributed to the presence of graphene layers which were modelled as a 'house of cards'. Oxidation of the carbon material leads to increased reversible capacity due to overall expansion of cavities and simultaneous increase in irreversible capacities in which lithium ions interact with oxide layers on the surface of carbon. The main drawback of carbonaceous materials prepared from phenolic resins is the higher discharge potential between charge–discharge cycles [156]. This phenomenon is observed particularly with carbonaceous materials which are heat-treated at lower temperature and is due to the interaction of Li^+ with C–H bonded sp^2 carbons on the edges and the formation of a stable sp^3 bonds [157]. Other recent studies support this view [158].

Improvements in the charge–discharge efficiency can be achieved by carefully eliminating inhibiting factors like hydrogen content, oxygen and oxide layers, as well as trace levels of water present in the carbonaceous materials [159]. Apart from phenolic resins [159], phenol–formaldehyde resin-based carbonaceous material was also found to give good lithium intercalation efficiency [160]. When heat-treated at 700 °C, this material gives a capacity of 438 mAh g^{-1} due to the formation of a polyacenic semiconductor [160]. Incorporation of phosphorous into phenolic resin material leads to the formation of carbon materials with nanostructures, which enhances the reversible capacity [161]. The phosphorous content and HTT procedure of this material also controls its overall performance [162].

Carbon materials prepared from PPP materials also exhibit fairly high reversible capacities of up to 710 mAh g^{-1} [163]. The HTT generally recommended for this material is in the range of 700 °C. Further incorporation of lithium up to a composition of LiC_2 is also possible [164]. At this stage, Li–Li metal bonding is observed [164]. Further increase in HTT can lead to a decrease in reversible capacity [165]. Detailed investigations suggest that beyond a composition of LiC_6, further incorporation of lithium ions occurs in the microcavities of the carbonaceous materials [166].

In contrast to an earlier view, PAN-based carbon anodes are also found to exhibit satisfactory performance provided the experimental conditions are properly optimised to achieve optimum fibre size as well as microporosity [167]. In addition to HTT [168], factors like heating rate and heating time [169] are also found to influence the electrochemical performance. Phosphorous doping is also found to improve the discharge capacity. The optimum HTT for PAN is found to be around 1000 °C while it is around 600 °C for phosphorous-doped PAN material [168,169].

A number of disordered-carbon materials have also been prepared from the pyrolysis of polymeric materials such as poly(2-chloro-1-phenylacetylene) [170], poly(vinylchloride) (PVC) [171,172], condensed poly-nuclear aromatics [173] and indoine blue [174]. Pyrolysis of 3,4,9,10-perylene-tetra-3,4,9,10-carboxylic anhydride gives perylene-based disordered-carbon material at around 55 °C [175,176]. Most of these materials provide higher levels of lithium doping beyond LiC_6. Nevertheless, the irreversible capacity remains high and the discharge voltage is substantially higher and gives rise to hysterisis in charge–discharge cycles. Carbonaceous materials prepared from metathesis of poly(butyne) were not found to be suitable for lithium insertion [177].

5.3. Carbonaceous materials from agricultural sources

Sugar is one of most widely studied sources for carbon-based host lattices for lithium. The influence of pyrolysis temperature and other operating parameters on the performance of this electrode material has been evaluated [178]. The irreversible capacity has been further reduced by optimising the HTT [179] and treating the hard carbon material with ethylene gas [180]. A much higher HTT leads to closing of micropores and the formation of fullerene-like structures and, hence, in an overall reduction in irreversible capacity [179]. Ball milling of the same sugar-based carbon materials leads to oxidised surface sites and, consequently, higher Q_{irr} [181].

A few other agricultural-based raw materials, such as rice husk [182], coffee beans, green tea, sugarcane [183] and cotton [184] have also been used to prepare active carbon materials and evaluate them for battery applications.

5.4. Synthetic carbons

Pyrolytic carbon materials prepared below 1200 °C have also been evaluated for their anode performance. Pyrolytic carbon prepared by chemical vapour deposition (CVD) of hydrocarbons was reported [185] to have shown up to 99% Columbic efficiency. More detailed investigations have indicated, however, the limitations of these material in terms of high discharge potentials and large hysterisis effects [186]. Thin films of carbon electrodes can be obtained by CVD through a plasma-enhanced method [187]. This type of anode material requires careful optimisation for potential applications for microbatteries [187]. CVD of pyridine and thiophene gives rise to pyrolytic carbon materials containing nitrogen and sulphur atoms, respectively. Such pyrolytic carbon materials containing and materials have been shown [188] to possess higher capacity depending on the conditions of preparation.

Quite recently, lithium insertion in carbon nanotubes and related materials has received some attention. Non-graphitic carbon nanotubes generally possess high irreversible capacity [189]. The conditions of preparation include the influence of the level of catalyst loading on the intercalation/de-intercalation behaviour [190]. During lithium intercalation, the crystalline structure is substantially modified and results

in capacity loss [191]. Electroless plating of copper on to the carbon nanotubes and subsequent oxidation to CuO does not lead to significant improvement in the anode behaviour [192]. Graphitized carbon nanotubes are shown, however, to give good reversible capacity [193]. The influence of the relative level of graphitization on the performance of carbon anodes has also been studied [53]. Naturally, a higher level of graphitization leads to better performance.

6. General conclusions and current trends

6.1. Carbon materials

The extensive survey presented above clearly indicates that synthetic graphite materials are currently dominating as commercially valuable anode materials. A few comparative investigations of different carbon materials by various research groups also confirm this view. Chusid et al. [194] have compared carbon black, hard carbon and synthetic graphite materials in a systematic way. They concluded that synthetic graphite with a relatively low level of crystal size gives best performance characteristics. Quite similar conclusions have been reached in a recent study [195] of different graphitic carbon electrodes. It is quite clear that large graphite crystals with a small total surface-area will have low irreversible capacity, while much smaller crystals with higher surface-area give a higher capacity loss due to SEI formation. Hence, an optimum crystalline size, which ensures optimum irreversible capacity while permitting the intercalation/de-intercalation process without exfoliation resulting in crystal breakdown is the basic requirement for a good battery material. Graphite particles with a standard size distribution, such as MCMB, MPCF and VGCF, thus, become the materials of choice as carbon anode [196,197]. Phosphorous doping [198] and silver incorporation [199] into such graphite particles also tend to improve anode performance. It seems possible to achieve good

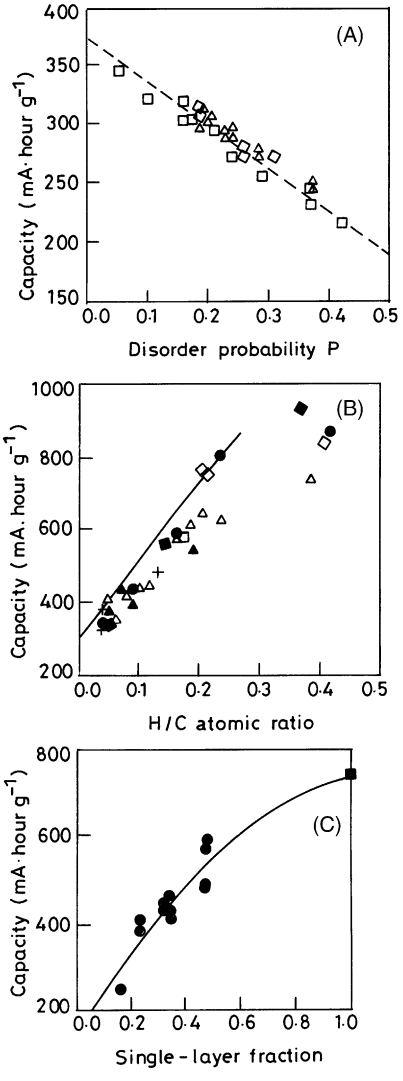

Fig. 7. Reversible capacity plotted as a function of: (A) probability (P) of turbostractic disorder between adjacent carbon sheets in region 1; (B) hydrogen content for different soft carbons heat-treated between 550 and 1000 °C in region 2; (C) single-layer fraction of epoxy resole resin [39] (for different regions, refer Fig. 2).

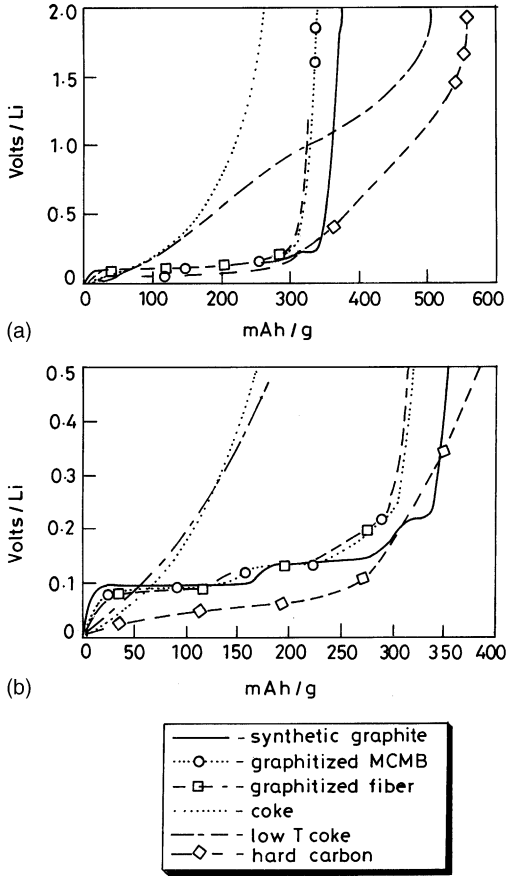

Fig. 8. Open-circuit voltage of fully lithiated carbon (short-circuit with lithium counter electrode for 48 h) as function of discharge capacity; (a) and (b) are the same figures at different scales to highlight the usable region. Electrolyte is EC/DMC 1 M $LiPF_6$ [9].

electrode performance by using natural graphite particles of optimum size and by ensuring their stability of coating with coke [200]. Nevertheless, the exact synthetic strategy adopted for the commercially successful anode material is not transparent.

Despite the predominance of synthetic graphite in commercial batteries, research efforts continue on all the three types of carbon materials, namely soft carbon, hard carbon and graphite materials (Fig. 2). The mechanistic pathways for incorporation of lithium ions in these materials are entirely different. Soft carbon materials contain C–H bonding with sp^2 hybridisation. Incorporation of lithium in this materials lead to sp^3 hybridisation of carbon and C···H–(···Li) bond formation. The materials serve as excellent reducing agents, but their discharge voltage is too low for them serve as anodes for batteries with high specific energy. As discussed extensively, intercalation of lithium into graphite occurs between the graphene layers and gives rise to an ideal LiC_6 structure. In hard carbon materials, lithium insertion occurs beyond LiC_6 or 372 mAh g^{-1} and depends on the fraction of single graphene layers that is present. Dahn et al. [39] clearly distinguished these three types of lithium insertion mechanism on carbon materials (Fig. 7). This shows the relationships between reversible capacity and turbostratic disorder in the graphite matrix, the H:C atomic ratio in soft carbon, and the single-layer fraction in the hard carbon, respectively. Comparison of the discharge capacity versus voltage profiles of different anode materials which range from synthetic carbon to hard carbon materials, is shown in Fig. 8 [9].

There is however, some interesting discussion on the exact model for intercalation of lithium ions in hard carbon materials. Buiel and Dahn [40] propose a 'house of card' model where each graphene plane is considered as a card. This model explains the variation of intercalation charge with HTT. Sato et al. [164] have advanced a predominantly adsorption-oriented model in which lithium–graphene layer interaction and Li–Li metallic interaction are considered separately. In the model presented by Mabuchi et al. [88], the excess capacity is mainly contributed by pores and voids in microcavities of disordered-carbon materials. Another recent model from Sony Corporation [41] considers two interactions, namely, pseudo-metallic lithium atom interaction with the graphene layer and a reducing force between

Table 3
Classification of different battery systems based on Wh capacity

Broad classification based on capacity	Company/association	Anode material	Individual discharge capacity (Wh)	Applications	Reference
Capacity below 10 Wh	LIBES, Japan				
	Matsushita CGR 17500	MCMB	3.4	Cellular phones, cameras and note-pads	[3,4]
	Sony US 18650	Coke	4.8	Cellular phones, cameras and note-pads	[3,4]
	Sanyo UR 18650	Coke + graphite	5.3	Cellular phones, cameras and note-pads	[200]
	Hitachi 18650	Resin	5.5	Cellular phones, cameras and note-pads	[206]
	Toshiba 863448	MCF	5.8	Cellular phones, cameras and note-pads	[204]
	A&T LSR 18650	MCF	5.9	Cellular phones, cameras and note-pads	[3,4]
	SAFT, France				
	MP 144350	Graphitized carbon	6.4	Space applications	[212]
Capacity above 10 Wh	LIBES, Japan				
	Toshiba	Hard carbon	10.6	Stationary and electric vehicle (EV)	[2]
	Sanyo	Coke + graphite	10.8	Stationary and electric vehicle (EV)	[2,207]
	Japan Storage Battery	Graphite	11.3	Stationary and electric vehicle (EV)	[3]
	Hitachi	Ag + graphite	11.8	Stationary and electric vehicle (EV)	[2,207]
	Mitsubishi Electric	MCMB	12.1	Stationary and electric vehicle (EV)	[2,207]
	Matsushita	Ga + carbon	14.7	Stationary and electric vehicle (EV)	[2,207]
	Nikkoso	VGCF	32.0	Stationary and electric vehicle (EV)	[205]
	YTP, US				
	Prismatic cell	MCMB	60	Military	[210]
Capacity above 100 Wh	LIBES, Japan				
	Hitachi and Shin-Kobe	Ag + graphite	250	Stationary	[207]
	Sanyo	Coke + graphite	270	Stationary	[208]
	Matsushita and Japan Storage	Graphite	370	Electric vehicle	[207]
	Mitsubishi	Graphite	400	Electric vehicle	[208]
	KERI, South Korea				
	Cylindrical cell	MCF	434	Electric vehicle	[213]
	SAFT, France				
	Prismatic prototype	MCF	460	Electric vehicle	[211]

the doped lithium atoms. Although some attempts towards quantifying these models are being made, there is still considerable uncertainty about the exclusive validation of any single mechanism.

6.2. Batteries

A large number of medium capacity, rechargeable batteries (<10 Wh) are now available commercially in the market (Table 3). Detailed specifications and performance characteristics of these commercial products are discussed in the literature by the respective manufacturers. The Sony Corporation, in 1991, employed coke as well as poly(furfurylalcohol) (PFA)-based hard carbon materials in its batteries [1,23,200]. Matsushita and Sanyo successfully used MCMB and a graphite + coke hybrid as the anode material in their batteries, respectively [25,201]. The performance characteristics of pitch-based, carbon fibre anodes in Li-ion batteries were well established in the mid-1990s [202,203]. Further, pitch-based carbon fibres and VGCF are the anode materials used by Toshiba and Nikkoso Corporation, respectively [204,205]. Hitachi, in an recent study, claimed [206] the use of phenolic resin-based hard carbon, as well as graphitized pitch-based coal-tar, as the host lattice [206]. Commercial batteries appear, however, to be employing silver dispersed graphite anodes (Table 3).

A comparative evaluation of battery constituents and performance characteristics of AA-type batteries from five different commercial sources has been reported quite recently [3,4]. A similar comparison of batteries in the medium prismatic range is also available [2]. The secondary batteries have already captured a substantial market share in mobile electronic equipment such as cellular phones and note-pads. There has been consistent and continuous growth in this segment in recent years.

At present, considerable research efforts are in progress to develop large-size, high capacity Li-on batteries throughout the world for applications that range from space, defence, electric vehicles and hybrid electric vehicles to large-scale stand-by applications. Batteries of 3–460 Wh capacity are under development according to available reports in the literature (Table 3). In Japan, the Lithium Battery Storage Technology Research Association (LIBES) is heading the standardisation of different classes of these batteries [2,12,207,208]. NASA is also sponsoring a large collaborative project in this area [13]. Other major companies heading this work are Yardney Technical Product (YTP) of US [209,210], SAFT of France [201,211,212] and the Korea Electrochemistry Research Institute (KERI) [213].

There appears to be considerable further scope for developing new and more efficient carbon anode material, as well as large-size secondary battery systems. Development of an alternative host lattice to replace carbon anodes appears to be far behind in the competitive race.

Acknowledgements

The authors wish to thank the Director, CECRI, Karaikudi for his constant encouragement and keen interest in this work. One of the authors, namely, V. Suryanarayanan, thanks CSIR, New Delhi for the award of a fellowship.

References

[1] T. Nagura, K. Tozawa, Prog. Batt. Solar Cells 9 (1990) 209.
[2] J. Aragane, K. Matsui, H. Andoh, S. Suzuki, H. Fukuda, H. Ikeya, K. Kitaba, R. Ishikawa, J. Power Sources 68 (1997) 13.
[3] B.A. Johnson, R.E. White, J. Power Sources 70 (1998) 48.
[4] R. Moshtev, B. Johnson, J. Power Sources 91 (2000) 86.
[5] Special issue on Li-ion insertion on host materials, Electrochim. Acta 45 (1999).
[6] Proceedings of 9th International Meeting on Lithium Batteries, Edinburgh, Scotland, UK, 12–17 July 1998, J. Power Sources 81/82 (1999).
[7] Proceedings of 10th International Meeting on Lithium Batteries, Como, Italy, 28 May–2 June 2000, J. Power Sources 97/98 (2001).
[8] J.O. Besenhard, in: W. Muller Warmuth, R. Schollorn (Eds.), Progress in Intercalation Research, Kluwer Academic Publishers, London, p. 282.
[9] M. Broussely, P. Biensan, B. Simon, Electrochim. Acta 45 (1999) 3.
[10] M. Broussely, J. Power Sources 81/82 (1999) 140.
[11] K. Tamura, T. Horiba, J. Power Sources 81/82 (1999) 156.
[12] T. Tanake, K. Ohta, N. Arai, J. Power Sources 97/98 (2001) 2.
[13] R.A. Marsh, S. Vukson, S. Surampudi, B.V. Ratnakumar, M.C. Smart, M. Manzo, P.J. Dalton, J. Power Sources 97/98 (2001) 25.
[14] K. Kinoshita, X. Song, J. Kim, M. Inaba, J. Power Sources 81/82 (1999) 170.
[15] Y. Hamon, T. Brousse, F. Jousse, P. Topart, P. Buvat, D.M. Schleich, J. Power Sources 97/98 (2001) 185.
[16] J. Chonvin, C. Branci, J. Sarradin, J. Oliver-Fourcade, J.C. Jumas, B. Simon, Ph. Biensan, J. Power Sources 81/82 (1999) 277.
[17] I. Exnar, L. Kavan, S.Y. Huang, M. Gretzel, J. Power Sources 68 (1997) 720.
[18] J.O. Besenhard, Carbon 14 (1976) 111.
[19] S. Basu, US Patent 4,304,825 (1981).
[20] S. Basu, US Patent 4,423,125 (1983).
[21] S. Basu, J. Power Sources 82 (1999) 200.
[22] R. Yazami, Ph. Touzain, J. Power Sources 9 (1983) 365.
[23] A. Kasei, US Patent 4,668,595 (1987).
[24] R. Fong, U. von Sacken, J.R. Dahn, J. Electrochem. Soc. 137 (1990) 2009.
[25] J. Yamanura, Y. Ozaki, A. Morita, A. Ohata, J. Power Sources 43 (1993) 233.
[26] S. Dresselhasu, G. Dresselhasu, K. Sugihare, I.L. Spain, H.A. Goldberg (Eds.), Cardona Manual, Graphite Fibres and Filaments, Springer, New York, 1988.
[27] K. Konishita, Carbon, Electrochemical and Physicochemical Properties, Wiley/Interscience, New York, 1988.
[28] A. Oberlin, in: P.A. Thrower (Ed.), Chemistry and Physics of Carbon, Vol. 22, V.1, Marcel Dekker, New York, 1989.
[29] F. Beck, in: R.C. Alkire, H. Gerischer, M. Kolb, C.W. Tobias (Eds.), Advances in Electrochemical Science and Engineering, Wiley, New York, 1997, p. 303.
[30] M. Noel, R. Santhanam, J. Power Sources 72 (1998) 53.
[31] D. Aurback (Ed.), Non-Aqueous Electrochemistry, Marcel Dekker, New York, 1999.
[32] N. Imanishi, Y. Takeda, O. Yamamoto, in: M. Wakihara, O. Yamamoto (Eds.), Lithium-ion Batteries, Fundamentals and Performance, Kodansha, Wiley, New York, 1988 (Chapter 5).

[33] T. Zheng, R. Dahn, Applications of carbon in lithium-ion batteries, in: T.D. Burchell (Ed.), Carbon Material of Advanced Technology, Pergamon Press, Oxford, UK, 1999.
[34] R. Yazami, in: C. Julien, Z. Stoyhov (Eds.), Materials for Li-ion Batteries, Kluwer Academic Publishers, London, 2000.
[35] D. Aurback, B. Markovsky, I. Weissman, E. Levi, Y.E. Eli, Electrochim. Acta 45 (1999) 67.
[36] D. Aurback, B. Markovsky, M.D. Levi, E. Levi, A. Schechter, M. Moshkovich, Y. Cohen, J. Power Sources 81/82 (1999) 95.
[37] R. Yazami, Electrochim. Acta 45 (1999) 87.
[38] R. Yazami, J. Power Sources 97/98 (2001) 33.
[39] J.R. Dahn, T. Zheng, Y. Liu, J.-S. Xue, Science 270 (1995) 590.
[40] E. Buiel, J.R. Dahn, Electrochim. Acta 45 (1999) 121.
[41] H. Azuma, H. Imoto, S. Yamada, K. Sekai, J. Power Sources 81/82 (1999) 1.
[42] M. Endo, C. Kim, K. Nishimura, T. Fujino, K. Miyashita, Carbon 38 (2000) 183.
[43] M. Morita, T. Ichimura, M. Ishikawa, Y. Matsuda, J. Power Sources 68 (1997) 253.
[44] T. Piano, S.-M. Park, C.-H. Don, S.-I. Moon, J. Electrochem. Soc. 146 (1999) 2794.
[45] A. Hamwi, Ph. Touzain, C. Reikel, Synth. Met. 7 (1983) 23.
[46] W. Metz, P. Josuks, V. Kiemman, Synth. Met. 7 (1983) 319.
[47] P. Behrens, W. Metz, Synth. Met. 23 (1988) 81.
[48] R. Santhanam, M. Noel, J. Power Sources 66 (1997) 47.
[49] Y. Maeda, Ph. Touzain, Electrochim. Acta 33 (1988) 1493.
[50] R. Santhanam, P. Kamaraj, M. Noel, J. Power Sources 72 (1999) 239.
[51] K. Suzuki, T. Iijima, M. Wakihara, Electrochim. Acta 44 (1999) 2185.
[52] M.D. Levi, D. Aurback, J. Phys. Chem. B 101 (1997) 4630.
[53] G.T. Wu, C.S. Wang, X.B. Zhang, H.S. Yang, Z.F. Qi, P.M. He, W.-Z. Li, J. Electrochem. Soc. 146 (1999) 1696.
[54] M. Inaba, Z. Siroma, Y. Kawatate, A. Funabiki, Z. Ogumi, J. Power Sources 68 (1997) 221.
[55] M. Inaba, Y. Kawatte, A. Funabiki, S.K. Jeong, T. Abe, Z. Ogumi, Electrochim. Acta 45 (1999) 99.
[56] F. Kong, R. Kostecki, G. Nadeau, X. Song, K. Zaghib, K. Kinoshita, F. McLarnon, J. Power Sources 97/98 (2001) 58.
[57] H. Ota, T. Sato, H. Suzuki, T. Usami, J. Power Sources 97/98 (2001) 107.
[58] Z. Ogurni, A. Sano, M. Inaba, T. Abe, J. Power Sources 97/98 (2001) 156.
[59] J.-C. Panitz, P. Novak, J. Power Sources 97/98 (2001) 174.
[60] D. Bar-Tow, E. Peled, L. Burstein, J. Electrochem. Soc. 146 (1999) 824.
[61] M.C. Smart, B.V. Ratnakumar, S. Surampudi, Y. Wang, X. Zhang, S.G. Greenbaum, A. Hightower, C.C. Ahn, B. Fultz, J. Electrochem. Soc. 146 (1999) 3963.
[62] K. Tatsumi, T. Akai, T. Imamura, K. Zaghib, N. Iwashita, S. Higuchi, Y. Sawada, J. Electrochem. Soc. 143 (1996) 1923.
[63] K. Zaghib, K. Tatsumi, Y. Sawada, S. Higuchi, H. Abe, T. Ohsaki, J. Electrochem. Soc. 146 (1999) 2784.
[64] K. Guerin, A.F. Bouvier, S. Flandrosis, M. Couzi, B. Simon, P. Biensan, J. Electrochem. Soc. 146 (1999) 3660.
[65] K. Zaghib, G. Nadeau, K. Kinoshita, J. Power Sources 97/98 (2001) 97.
[66] J.P. Oliver, M. Winter, J. Power Sources 97/98 (2001) 151.
[67] F. Joho, B. Rykart, A. Blome, P. Novak, H. Wilhelm, M.E. Spahr, J. Power Sources 97/98 (2001) 78.
[68] V. Suryanarayanan, M. Noel, J. Power Sources 94 (2001) 137.
[69] R. McMillan, H. Slegr, Z.X. Shu, W. Wang, J. Power Sources 81/82 (1999) 20.
[70] G.H. Wrodnigg, J.O. Besenhard, M. Winter, J. Electrochem. Soc. 146 (1999) 470.
[71] D. Zane, A. Antonini, M. Pasquali, J. Power Sources 97/98 (2001) 146.
[72] K. Edstrom, A.M. Andersson, A. Bishop, L. Fransson, J. Lindgren, A. Hussenius, J. Power Sources 97/98 (2001) 87.
[73] G.B. Appetecchi, F. Croce, R. Marassi, L. Persi, P. Romagholi, B. Scrosati, Electrochim. Acta 45 (1999) 23.
[74] D. Aurback, A. Zaban, Y.E. Eli, L. Weissman, O. Chusid, O.A. Abramson, B. Markovsky, J. Power Sources 54 (1995) 78.
[75] A. Naji, J. Ghanbaja, P. Willmann, D. Billaud, J. Power Sources 81/82 (1999) 207.
[76] M. Dolle, S. Grugeon, B. Beaudoin, L. Dupond, J.-M. Tarascon, J. Power Sources 97/98 (2001) 104.
[77] P. Novak, F. Joho, M. Lanz, B. Rykart, J.-C. Panifz, D. Alliata, R. Kotz, O. Haas, J. Power Sources 97/98 (2001) 39.
[78] A. Martinent, B.L. Gorrec, C. Montella, R. Yazami, J. Power Sources 97/98 (2001) 83.
[79] C. Wang, A.J. Appleby, F.E. Little, Electrochim. Acta 46 (2001) 1793.
[80] C. Bindra, V.A. Nalimova, D.E. Sklovsky, Z. Benes, J.E. Fischer, J. Electrochem. Soc. 145 (1998) 2377.
[81] E. Peled, D. Bar-Tow, A. Merson, A. Gladkich, L. Burstein, D. Golodnitsky, J. Power Sources 97/98 (2001) 52.
[82] F. Funabiki, M. Inaba, Z. Ogumi, J. Power Sources 68 (1997) 227.
[83] A. Funabiki, M. Inaba, T. Abe, Z. Ogurni, Electrochim. Acta 45 (1999) 865.
[84] F. Funabiki, M. Inaba, T. Abe, Z. Ogurni, J. Electrochem. Soc. 146 (1999) 2443.
[85] C. Lampe-Onnerud, J. Shi, P. Onnerud, R. Charnberlain, B. Barnett, J. Power Sources 97/98 (2001) 133.
[86] Y. Korai, S. Ishida, S.H. Yoon, I. Mochida, Y. Nakagawa, C.Y. Matsumura, Y. Sakai, M. Komatu, Carbon 35 (1999) 1503.
[87] Y.C. Chang, H.J. Sonu, C.-H. Ku, Y.G. Wang, Y. Korai, I. Mochida, Carbon 37 (1999) 1285.
[88] A. Mabuchi, K. Tokumitsu, H. Fujimoto, T. Kasuh, J. Electrochem. Soc. 142 (1995) 1041.
[89] T. Kasuh, A. Mabuchi, K. Tokumitsu, H. Fujimoto, J. Power Sources 68 (1997) 99.
[90] K. Tatsumi, N. Iwashita, H. Sakaebe, H. Shioyama, S. Higuchi, A. Mabuchi, F. Fujimoto, J. Electrochem. Soc. 142 (1995) 716.
[91] A. Mabuchi, H. Fujimoto, K. Tokumitsu, T. Kasuh, J. Electrochem. Soc. 142 (1995) 3049.
[92] K. Suzuki, T. Hamada, T. Sugiura, J. Electrochem. Soc. 146 (1999) 890.
[93] W. Xing, J.R. Dahn, J. Electrochem. Soc. 144 (1997) 1195.
[94] C. Yuqin, L. Hong, W. Lie, L. Tianhong, J. Power Sources 68 (1997) 187.
[95] T. Zheng, A.S. Gozdz, G.G. Amatucci, J. Electrochem. Soc. 146 (1999) 4014.
[96] C.R. Yang, Y.Y. Wang, C.C. Wan, J. Power Sources 72 (1998) 66.
[97] Y.C. Chang, H.J. Sohn, J. Electrochem. Soc. 147 (2000) 50.
[98] M.N. Richard, J.R. Dahn, J. Power Sources 83 (1999) 71.
[99] K. Zaghib, K. Tatsurni, H. Abe, T. Ohsaki, Y. Sawada, S. Higuchi, J. Electrochem. Soc. 145 (1998) 210.
[100] K. Tatsumi, K. Zaghib, Y. Sawada, H. Abe, T. Ohsaki, J. Electrochem. Soc. 142 (1999) 1090.
[101] K. Yamaguchi, J. Suzuki, M. Saito, K. Sekine, T. Takamure, J. Power Sources 97/98 (2001) 159.
[102] N. Imanishi, H. Kashiwagi, T. Ichigawa, Y. Takeda, O. Yamamoto, M. Inagaki, J. Electrochem. Soc. 140 (1993) 315.
[103] T. Uchida, Y. Morikawa, H. Ikota, M. Wakihara, K. Suzuki, J. Electrochem. Soc. 143 (1996) 2606.
[104] Y. Sato, T. Nakano, K. Kobayakawa, T. Kawai, A. Yokoyama, J. Power Sources 75 (1998) 271.
[105] T.D. Tran, D.J. Derwin, P. Zaleski, X. Song, K. Kinishita, J. Power Sources 81/82 (1999) 296.
[106] Q.-M. Pan, Z.-H. Deng, X.-Z. Zhang, G.-X. Wan, J. Power Sources 79 (1999) 25.
[107] H. Wang, T. Ikeda, K. Fukuda, M. Yoshio, J. Power Sources 83 (1999) 141.

[108] F. Disma, L. Aymard, L. Dupont, J.-M. Tarascon, J. Electrochem. Soc. 143 (1996) 3959.
[109] F. Salver-Disma, A. Dupasquier, J.-M. Tarascon, J.-S. Lassegues, J.-N. Rouzaud, J. Power Sources 81/82 (1999) 291.
[110] C.S. Wang, G.T. Wu, W.-Z. Li, J. Power Sources 76 (1998) 1.
[111] T.D. Tran, L.M. Speilman, W.M. Goldberg, X. Song, K. Kinoshita, J. Power Sources 68 (1997) 106.
[112] B. Simons, S. Flandrois, K. Guerin, A. Fevrier-Bouvier, I. Teulet, P. Biensan, J. Power Sources 81/82 (1999) 312.
[113] K. Fukuda, K. Kikuya, K. Isono, M. Yoshio, J. Power Sources 69 (1997) 165.
[114] H. Buqa, P. Golob, M. Winter, J.O. Besenhard, J. Power Sources 97/98 (2001) 122.
[115] R. Tossici, M. Berrettoni, M. Roseleu, R. Marassi, B. Scrosati, J. Electrochem. Soc. 144 (1997) 186.
[116] Y. Matsuo, Y. Sugie, J. Electrochem. Soc. 146 (1999) 2011.
[117] T. Takamura, M. Saito, A. Shimokawa, C. Nakahara, K. Sekine, S. Maeno, N. Kibayashi, J. Power Sources 90 (2000) 45.
[118] S. Yoon, H. Kim, S.M. Oh, J. Power Sources 94 (2001) 68.
[119] J. Drofenik, M. Gaberscek, R. Dominko, M. Bele, S. Pejovnik, J. Power Sources 94 (2001) 97.
[120] M. Gaberscek, M. Bele, J. Drofenik, R. Dominko, S. Pejovnik, J. Power Sources 97/98 (2001) 67.
[121] H. Buqa, Ch. Grogger, M.V. Santis Alverz, J.O. Besenhard, M. Winter, J. Power Sources 97/98 (2001) 126.
[122] S.B. Ng, J.-Y. Lee, Z.L. Liu, J. Power Sources 94 (2001) 63.
[123] M. Endo, C. Kim, T. Karaki, Y. Nishimura, M.J. Mattew, S.D.M. Brown, M.S. Dresselhaus, Carbon 37 (1999) 561.
[124] C. Kim, T. Fujino, T. Hayashi, M. Endo, M.S. Dresselhaus, J. Electrochem. Soc. 147 (2000) 1265.
[125] B.M. Way, J.R. Dahn, J. Electrochem. Soc. 141 (1994) 907.
[126] W.J. Weydanz, B.M. Way, T. Van Buuren, J.R. Dahn, J. Electrochem. Soc. 141 (1994) 900.
[127] H. Hwang, E.M. Kelder, J. Schoonman, J. Power Sources 94 (2001) 108.
[128] C. Kim, T. Fujino, K. Miyasnita, T. Hayashi, M. Endo, M.S. Dresselhaus, J. Electrochem. Soc. 147 (2000) 1257.
[129] A.M. Wilson, J.R. Dahn, J. Electrochem. Soc. 142 (1995) 327.
[130] Y. Wu, S. Fang, W. Ju, Y. Jiang, J. Power Sources 70 (1998) 114.
[131] J.-Y. Lee, R. Zhang, Z. Liu, J. Power Sources 90 (2000) 70.
[132] J.-Y. Lee, R. Zhang, Z. Liu, Electrochem. Solid State Lett. 3 (2000) 167.
[133] T. Takamura, J. Suzuki, C. Yamada, K. Sumiya, K. Sekine, Surf. Energy 15 (1999) 225.
[134] T. Takamura, K. Sumiya, J. Suzuki, C. Yamada, K. Sekine, J. Power Sources 81/82 (1999) 368.
[135] F. Joho, B. Ryhart, R. Imhof, P. Novak, M.E. Spahr, A. Monnier, J. Power Sources 81/82 (1999) 243.
[136] Z. Liu, A. Yu, J.-Y. Lee, J. Power Sources 81/82 (1999) 187.
[137] H. Huang, E.M. Kelder, J. Schoonman, J. Power Sources 97/98 (2001) 114.
[138] M. Jean, A. Chausse, R. Messina, J. Power Sources 68 (1997) 232.
[139] B. Laik, F. Gessier, F. Mercier, P. Trocellier, A. Chausse, R. Messina, Electrochim. Acta 44 (1999) 1667.
[140] H. Laik, A. Chausse, R. Messina, M.G. Barthes-Labrousse, J.Y. Nedelec, C. Le Paven-Thivet, F. Grillon, Electrochim. Acta 46 (2000) 691.
[141] G. Okuna, K. Kobayakawa, Y. Sato, T. Kawai, A. Yokoyama, Denki Kagak 65 (1997) 226.
[142] Y. Sato, K.-I. Tannma, T. Takayama, K. Kobayakawa, T. Kawai, A. Yokoyama, J. Power Sources 97/98 (2001) 165.
[143] R. Yazami, K. Zaghib, M. Deschamps, J. Power Sources 52 (1994) 55.
[144] M. Deschamps, R. Yazami, J. Power Sources 68 (1997) 236.
[145] Y.B. Roh, K.M. Jeong, H.G. Cho, H.Y. Kang, Y.S. Lee, S.K. Ryu, B.S. Lee, J. Power Sources 8 (1997) 271.
[146] J.-S. Kim, J. Power Sources 97/98 (2001) 70.
[147] I. Mochida, C.-H. Ku, S.H. Yoon, T. Korai, J. Power Sources 75 (1998) 214.
[148] K. Tatsumi, T. Kawamura, S. Higuchi, S. Hosotubo, H. Nakajuma, Y. Sawada, J. Power Sources 68 (1997) 263.
[149] S. Wang, S. Yata, J. Nagano, Y. Okano, H. Kinoshita, H. Kikuta, T. Yamabe, J. Electrochem. Soc. 147 (2000) 2498.
[150] A. Larcher, C. Mudalige, M. Gharghouri, J.R. Dahn, Electrochim. Acta 44 (1999) 4069.
[151] M. Saito, K. Sumiya, K. Sekine, T. Takamura, Electrochemistry 67 (1999) 957.
[152] S.J. Lee, M. Nishizawa, I. Uchida, Electrochim. Acta 44 (1999) 2379.
[153] E. Frackowiak, J. Machinikowski, H. Kaczmarska, F. Beguin, J. Power Sources 97/98 (2001) 140.
[154] J.-S. Xue, J.R. Dahn, J. Electrochem. Soc. 142 (1995) 3668.
[155] Y. Liu, J.-S. Xue, T. Zheng, J.R. Dahn, Carbon 34 (1996) 193.
[156] T. Zheng, Q. Zhong, J.R. Dahn, J. Electrochem. Soc. 142 (1995) L 211.
[157] T. Zheng, W.R. Mckinnon, J.R. Dahn, J. Electrochem. Soc. 143 (1996) 2137.
[158] Z. Wang, X. Huang, L. Chen, J. Power Sources 81/82 (1999) 328.
[159] T. Takamura, H. Awano, T. Ura, K. Sumiya, J. Power Sources 68 (1997) 114.
[160] B. Huang, Y. Huang, Z. Wang, L. Chen, R. Xue, F. Wang, J. Power Sources 58 (1996) 231.
[161] H.H. Schonfelder, K. Kitoh, H. Nemoto, J. Power Sources 68 (1997) 258.
[162] H.-Q. Xiang, S.-B. Fang, Y.-Y. Jiang, J. Power Sources 94 (2001) 85.
[163] M. Alamgir, Q. Zuo, K.M. Abraham, J. Electrochem. Soc. 141 (1994) L 143.
[164] K. Sato, M. Noguchi, A. Demachi, N. Oki, M. Endo, Science 64 (1994) 556.
[165] J. Gong, H. Wu, Q. Yang, Carbon 37 (1999) 1409.
[166] J. Gong, H. Wu, Electrochem. Acta 45 (2000) 1753.
[167] M.W. Verbrugge, B.J. Koch, J. Electrochem. Soc. 143 (1996) 24.
[168] Y. Jung, M.C. Suh, H. Lee, M. Kim, S.I. Lee, S.C. Shim, J. Kwak, J. Electrochem. Soc. 144 (1997) 4279.
[169] Y. Wu, S. Fang, Y. Jiang, J. Power Sources 75 (1998) 201.
[170] R. Kanno, Y. Takeda, T. Ichikawa, R. Nakanishi, O. Yamamoto, J. Power Sources 26 (1989) 535.
[171] T. Zheng, Y. Liu, E.W. Fuller, S. Tseng, U. von Sacken, J.R. Dahn, J. Electrochem. Soc. 142 (1995) 2581.
[172] T. Zheng, J.R. Dhan, J. Power Sources 68 (1997) 201.
[173] K. Tokumistsu, A. Mabuchi, H. Fujumoto, T. Kasuh, J. Electrochem. Soc. 43 (1996) 2235.
[174] L. Duclaux, E. Frackowiak, F. Beguin, J. Power Sources 81/82 (1999) 323.
[175] N. Takami, A. Satoh, T. Ohsaki, M. Kanada, J. Electrochem. Soc. 145 (1998) 478.
[176] N. Takami, A. Satoh, M. Oguchi, H. Sasaki, T. Ohsaki, J. Power Sources 68 (1997) 283.
[177] Y. Jung, M. Suh, S.C. Shim, T. Kwak, J. Electrochem. Soc. 145 (1998) 3123.
[178] W. Xing, J.-S. Xue, J.R. Dahn, J. Electrochem. Soc. 143 (1996) 3046.
[179] E. Buiel, A.E. George, J.R. Dahn, J. Electrochem. Soc. 145 (1998) 2252.
[180] E. Buiel, J.R. Dahn, J. Electrochem. Soc. 145 (1998) 1977.
[181] W. Xing, R.A. Dunlap, J.R. Dahn, J. Electrochem. Soc. 145 (1998) 62.
[182] G.T.K. Fey, C.-L. Chen, J. Power Sources 97/98 (2001) 47.
[183] S.-I. Yamada, H. Imoto, K. Sekai, M. Nagamine, Proceedings of the Electrochemical Society Spring Meeting, Montreal, Quebec, Canada, May 1997, The Electrochemical Society Inc., Pennington, NJ, Extended Abstracts, Vol. 97-1, p. 85.
[184] V. Eskenaziand, E. Peled, Proceedings of the Electrochemical Society Fall Meeting, San Antonio, TX, October 1996, The

Electrochemical Society Inc., Pennington, NJ, Extended Abstracts, Vol. 96-2, p. 1051.
[185] M. Mohri, N. Yanagiasawa, T. Tajima, H. Tanaka, T. Mitate, S. Nakajima, M. Yoshida, Y. Yoshimoto, T. Suzuki, H. Wada, J. Power Sources 26 (1989) 545.
[186] Y.-S. Han, J.-S. Yu, G.-S. Park, J.-Y. Lee, J. Electrochem. Soc. 146 (1999) 3999.
[187] S.I. Pyun, S.J. Orr, J. Mater. Sci. Lett. 18 (1999) 591.
[188] S. Ito, T. Murata, M. Hasegawa, Y. Bito, Y. Toyoguchi, J. Power Sources 68 (1997) 245.
[189] F. Leroux, K. Meternier, S. Gautier, E. Frackowiak, S. Bonnamy, F. Beguin, J. Power Sources 81/82 (1999) 317.
[190] T. Ishihara, A. Kawahare, H. Nishiguchi, M. Yoshio, Y. Takita, J. Power Sources 97/98 (2001) 129.
[191] A.S. Claye, J.E. Fischer, C.B. Huffman, A.G. Rinzler, R.E. Smalley, J. Power Sources 147 (2000) 2845.
[192] G.T. Wu, C.S. Wang, X.B. Zhang, H.S. Yang, Z.F. Qi, W.-Z. Li, J. Power Sources 75 (1998) 175.
[193] T. Ishihara, A. Fukinaga, R. Akiyoshi, M. Yoshio, Y. Takita, Electrochemistry 68 (2000) 38.
[194] O. Chusid, Y.E. Ely, D. Aurback, M. Babai, Y. Carmali, J. Power Sources 43/44 (1993) 47.
[195] G.-C. Chung, S.H. Jun, K.Y. Lee, M.H. Kim, J. Electrochem. Soc. 146 (1999) 1664.
[196] N. Takaini, A. Satoh, M. Hara, T. Ohsaki, J. Electrochem. Soc. 142 (1995) 371.
[197] C. Yuqin, L. Hong, W. Lie, L. Tianhong, J. Power Sources 68 (1997) 187.
[198] T. Tran, J. Feikert, X. Song, K. Kinoshita, J. Electrochem. Soc. 142 (1995) 3297.
[199] H. Honbo, S. Takeuchi, H. Momose, K. Nishimura, T. Horiba, Y. Muranaka, R. Kozono, Denki Kagaku 66 (1999) 239.
[200] K. Sekai, H. Azuma, A. Omaru, S. Fujita, H. Imoto, T. Endo, I. Yamaura, I. Nishi, H. Mashiko, M. Yokogewa, J. Power Sources 43/44 (1993) 241.
[201] Y. Kida, K. Yanagida, A. Funahashi, T. Nohma, I. Yoneza, J. Power Sources 94 (2001) 74.
[202] M. Morita, N. Nishimura, Y. Matsuda, Electrochem. Acta 38 (1993) 1721.
[203] N. Takarni, A. Satoh, M. Hara, T. Ohaski, J. Electrochem. Soc. 142 (1995) 2564.
[204] T. Ohsaki, M. Kanda, Y. Aoki, H. Shiroki, S. Suzuki, J. Power Sources 68 (1997) 102.
[205] H. Abe, T. Murai, K. Zaghib, J. Power Sources 77 (1999) 110.
[206] H. Higuchi, K. Uenae, A. Kawakarni, J. Power Sources 68 (1997) 212.
[207] T. Iwahori, Y. Ozaki, A. Funahashi, H. Momose, I. Mitsuishi, S. Shiraga, S. Yoshitake, H. Awata, J. Power Sources 81/82 (1999) 872.
[208] K. Tamura, T. Horiba, J. Power Sources 81/82 (1999) 156.
[209] G.M. Ehrlich, F.J. Puglia, R.L. Gitzendanner, B. Hellen, C. Marsh, J. Power Sources 81/82 (1999) 863.
[210] R.L. Gitzendanner, P.G. Russell, C. Marsh, R.A. Marsh, J. Power Sources 81/82 (1999) 847.
[211] M. Broussely, J.P. Planchat, G. Rigobent, D. Virey, G. Sarre, J. Power Sources 68 (1997) 8.
[212] M. Brousely, J. Power Sources 81/82 (1999) 140.
[213] Y.-E. Hyung, S.-I. Moon, D.-H. Yum, S.-K. Yun, J. Power Sources 81/82 (1999) 842.